# LEVERAGING CLASS HIERARCHIES WITH METRIC-GUIDED PROTOTYPE LEARNING

**Anonymous authors**
Paper under double-blind review

## ABSTRACT

Not all errors are created equal. This is especially true for many key machine learning applications. In the case of classification tasks, the severity of errors can be summarized under the form of a *cost matrix*, which assesses the gravity of confusing each pair of classes. When the target classes are organized into a hierarchical structure, this matrix defines a metric. We propose to integrate this metric in a new and versatile classification layer in order to model the disparity of errors. Our method relies on jointly learning a feature-extracting network and a set of class representations, or *prototypes*, which incorporate the error metric into their relative arrangement in the embedding space. Our approach allows for consistent improvement of the severity of the network's errors with regard to the cost matrix. Furthermore, when the induced metric contains insight on the data structure, our approach improves the overall precision as well. Experiments on four different public datasets—from agricultural time series classification to depth image semantic segmentation—validate our approach.

## 1 INTRODUCTION

The errors of critical systems such as autonomous navigation can range from benign to dramatic, *e.g.* confusing a car with a van *vs.* a street lamp with a crossing pedestrian. However, this error discrepancy is not taken into account by most classification algorithms, neither in the chosen loss functions nor the evaluation metrics. Criticisms of neural networks have also targeted their tendency to produce improbable yet confident errors, notably when attacked (Akhtar & Mian, 2018). A step towards more reliable and interpretable algorithms would be to explicitly model that some class confusions are less acceptable than others.

For a classification task over a set $\mathcal{K}$ of $K$ classes, this hierarchy of errors can be encapsulated by a cost matrix $D \in \mathbb{R}_+^{K \times K}$, defined such that the cost of predicting class $k$ when the true class is $l$ is $D[k, l] \geq 0$, and $D[k, k] = 0$. In this paper, we also assume that $D$ respects the triangle inequality: $D[k, l] + D[l, m] \geq D[k, m]$ for all $k, l, m$ in $\mathcal{K}$. A prominent setting in which such matrix can be constructed is when the set of classes $\mathcal{K}$ is organized according to a tree-shaped hierarchy. Among many other options (Kosmopoulos et al., 2015), one can define $D[k, l]$ as the length of the shortest path between the nodes corresponding to classes $k$ and $l$. Such tree-shaped taxonomy of concepts can be generated by domain experts, or automatically from class names with the WordNet graph (Miller et al., 1990) or word embeddings (Mikolov et al., 2013) for example.

As pointed out by Bertinetto et al. (2020), the first step towards algorithms aware of error costs would be to generalize the use of cost-based metrics. For example, early iterations of the ImageNet challenge (Russakovsky et al., 2015; Deng et al., 2010) proposed to weight errors according to hierarchy-based costs. For a dataset indexed by $\mathcal{N}$, the *Average Cost* (AC) between class predictions $y \in \mathcal{K}^{\mathcal{N}}$ and the true labels $z \in \mathcal{K}^{\mathcal{N}}$ is defined as:

$$\text{AC}(y, z) = \frac{1}{|\mathcal{N}|} \sum_{n \in \mathcal{N}} D[y_n, z_n] \ . \tag{1}$$

Along with evaluation metrics, loss functions should also take the cost matrix into account. While it is common to focus on retrieving certain classes through weighting schemes, preventing specific class confusions is less straightforward. The cross entropy for example singles out the prediction with respect to the correct class, but treats all other classes equally.

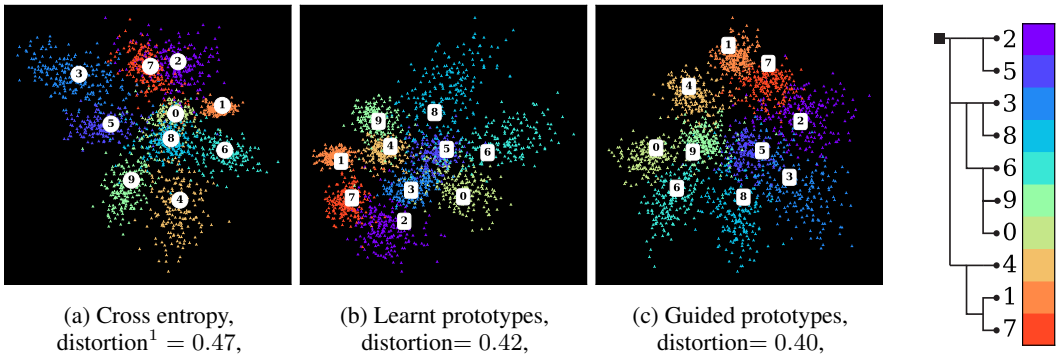


(a) Cross entropy, distortion[1] $= 0.47$, ER$= 15.2\%$, AC $= 0.81$

(b) Learnt prototypes, distortion$= 0.42$, ER$= 14.2\%$, AC $= 0.75$

(c) Guided prototypes, distortion$= 0.40$, ER$= 11.9\%$, AC $= 0.52$

Figure 1: Mean class representation ○ , prototypes □ , and 2-dimensional embeddings ⅄ learnt on perturbed MNIST by a 3-layer convolutional net with three different classification modules: (a) cross-entropy, (b) learnt prototypes, and (c) learnt prototypes guided by a tree-shaped taxonomy (constructed according to the authors' perceived visual similarity between digits). The guided prototypes (c) have lower distortion[1] with respect to the tree-induced metric: classes with low error cost are closer. This is associated with a decrease in the *Average Cost* (AC), as well as *Error Rate* (ER), indicating that our taxonomy may contain useful information for learning better visual features.

Beyond reducing the AC, another advantage of incorporating the cost matrix into the learning phase is that $D$ may contain information about the structure of the data as well. Though it is not always the case, pairs of classes with low associated cost tend to share some structural properties. Encouraging such classes to have similar representations could lead to more efficient learning, *e.g.* by pooling common feature detectors. Such priors on the class structure may be especially crucial when dealing with a large taxonomy, as noted by Deng et al. (2010).

In this paper, we introduce a method to integrate the cost of errors into a classification algorithm. Our approach relies on a new variation of prototypical networks (Snell et al., 2017; Dong & Xing, 2018), in which class prototypes are learnt jointly with the embedding network, in an end-to-end fashion. This allows us to integrate the cost matrix, interpreted as a finite metric over $\mathcal{K}$, into a regularizing function in order to organize the prototypes such that their relative distances reflect the cost of misclassifying their respective classes.

The contributions of this paper are as follows:

- We introduce a new formulation of prototypical networks in which the prototypes are learnt conjointly to the embedding network.
- We incorporate the error hierarchy through a penalization based on our scale-independent formulation of the distortion between two metric spaces.
- We show on four public datasets (CIFAR100 , NYUDv2, S2-Agri, and iNaturalist-19) that our approach decreases the average cost of the prediction of standard backbones.
- As illustrated in Figure 1, we show that our approach can also lead to a better (unweighted) precision, which we attribute to useful priors contained in the taxonomy of classes.

## 2 Related Work

**Prototypical Networks:** Our approach builds on the growing corpus of work on prototypical networks. These models are deep learning analogues of nearest centroid classifiers (Tibshirani et al., 2002), which associate to each class a representation, or prototype, and classify observations according to the nearest prototype. These networks have been successfully used for few-shot learning (Snell et al., 2017; Dong & Xing, 2018), zero-shot learning (Jetley et al., 2015), and supervized classification (Guerriero et al., 2018; Mettes et al., 2019).

[1] Scale-free distortion, see Section 3.2; computed from the means of class embeddings for the cross entropy.

In most approaches, the prototypes are directly defined as the centroid of the learnt representations of samples of their classes, and updated at each episode (Snell et al., 2017) or iteration (Guerriero et al., 2018). In the work of Mettes et al. (2019) and Jetley et al. (2015), the prototypes are defined prior to learning the embedding function. In contrast, we propose to view the prototypes as trainable parameters to be learnt simultaneously to the data embedding function.

**Hierarchical Priors:** The idea of exploiting the latent taxonomic structure of semantic classes in order to improve the accuracy of a model has been extensively explored (Silla & Freitas, 2011), from traditional Bayesian modeling (Gelman et al., 2013, Chapter 5) to adaptive deep learning architectures (Yan et al., 2015; Roy et al., 2020; Salakhutdinov et al., 2012; Ayub & Saini, 2011). However, for these neural networks, the hierarchy is discovered by the network itself in the goal of improving the overall accuracy of the model. In our setting, the hierarchy is defined a priori, and serves both to evaluate the quality of the model and to guide the learning process towards a reduced prediction cost.

Srivastava & Salakhutdinov (2013) propose implementing Gaussian priors on the weight of neurons according to a fixed hierarchy. Redmon & Farhadi (2017) implement an inference scheme based on a tree-shaped graphical model derived from a class taxonomy. Closest to our work, Hou et al. (2016) propose a regularization based on the earth mover distance to penalize errors with high costs.

More recently, Bertinetto et al. (2020) highlighted the relative lack of well-suited methods for dealing with hierarchical nomenclatures in the deep learning literature. They advocate for a more widespread use of the AC for evaluating models, and detail two simple baseline classification modules able to decrease the AC of deep models: *Soft-Labels* and *Hierarchical Cross-Entropy*. See Section 4.3 for more details on these schemes.

**Finite Metric Embeddings:** Our objective of computing class representations with pairwise distances determined by a cost matrix has links with finding an isometric embedding of the cost matrix—seen as a finite metric. This problem has been extensively studied (Indyk et al., 2017; Bourgain, 1985) and is at the center of the growing interest for hyperbolic geometry (De Sa et al., 2018). However, our goal is simply to influence the learning of prototypes with a metric rather than necessarily seeking the best possible isometry.

## 3 METHOD

We consider a generic dataset $\mathcal{N}$ of $N$ elements $x \in \mathcal{X}^{\mathcal{N}}$ with ground truth classes $z \in \mathcal{K}^{\mathcal{N}}$. We assume that the cost matrix $D \in \mathbb{R}_+^{K \times K}$ is symmetric, *i.e.* misclassifying class $k$ for class $l$ or the contrary has the same cost. We also assume that $D$ respects the triangle inequality and thus that $(\mathcal{K}, D)$ defines a finite metric space. Cost matrices which do not respect these two conditions are out of the scope of this paper. We denote by $\Omega$ the *embedding space* which, when equipped with the distance function $d : \Omega \times \Omega \mapsto \mathbb{R}_+$, forms a metric space as well.

### 3.1 PROTOTYPICAL NETWORKS

A prototypical network is characterized by an embedding function $f : \mathcal{X} \mapsto \Omega$, typically a neural network, and a set $\pi \in \Omega^{\mathcal{K}}$ of $K$ prototypes. $\pi$ must be chosen such that any sample $n$ of a given class $k$ has a representation $f(x_n)$ which is *close* to $\pi_k$ and *far* from other prototypes.

Following the methodology of Snell et al. (2017), a prototypical network $(f, \pi)$ associates to an observation $x_n$ the following posterior distribution over its class $z_n$:

$$p(z_n = k | x_n) = \frac{\exp\left(-d\left(f(x_n), \pi_k\right)\right)}{\sum_{l \in \mathcal{K}} \exp\left(-d\left(f(x_n), \pi_l\right)\right)} \, , \forall k \in \mathcal{K} \, . \tag{2}$$

We can then define an associated loss with the normalized negative log-likelihood of the true classes:

$$\mathcal{L}_{\text{data}}(f, \pi) = \frac{1}{N} \sum_{n \in \mathcal{N}} \left( d(f(x_n), \pi_{z_n}) + \log \left( \sum_{l \in \mathcal{K}} \exp\left(-d(f(x_n), \pi_l)\right) \right) \right) \, . \tag{3}$$

This loss is such that the representation $f(x_n)$ is attracted towards the prototype of the class $z_n$, while it is repelled by the other prototypes. Conversely, prototype $\pi_k$ is drawn towards the representations $f(x_n)$ of samples $n$ of class $k$ and away from the representations of other classes.

In contrast to previous work on prototypical networks which learn prototypes separately or define them as centroids of representations, we propose to learn the embedding function $f$ and the prototypes $\pi$ *simultaneously*. This allows us to learn prototypes which take into account both the distribution of the data and the relationships between classes, as described in the next section. Furthermore, this removes the need for keeping track of the average representation of each class.

### 3.2 Metric-Guided Penalization

We propose to incorporate the cost matrix $D$ into a regularization term in order to encourage the prototypes to organize in the embedding space $\Omega$ in a manner that is consistent with the finite metric defined by $D$. Since sample representations are attracted to their respective prototypes in (3), this regularization also affects the embedding network.

**Scale-Free Distortion** As described in De Sa et al. (2018), the distortion of a mapping $k \mapsto \pi_k$ between the finite metric space $(\mathcal{K}, D)$ and the continuous metric space $(\Omega, d)$ can be defined as:

$$\text{disto}(\pi, D) = \frac{1}{K(K-1)} \sum_{k,l \in \mathcal{K}^2,\, k \neq l} \frac{|d(\pi_k, \pi_l) - D[k,l]|}{D[k,l]} \,. \tag{4}$$

If the prototypes $\pi$ define a low-distortion mapping, their pairwise distances $d$ are close to the misclassification costs defined by $D$. Consequently, for a sample $x_n$ of true class $k$ to be misclassified with a high cost class $l$ (with high $D[k,l]$), the distance between the representation $f(x_n)$ and the correct prototype $\pi_k$ must be large. In contrast, errors with a lower cost can take place with a smaller erroneous offset. Therefore, prototypes arrangements with low distortion may be less prone to high-cost misclassifications, and thus be advantageous in terms of AC.

However, achieving low-distortion also imposes a specific scale on the distances between prototypes in the embedding space. This scale may conflict with the second term of $\mathcal{L}_{\text{data}}$ which encourages distances between embeddings and unrelated prototypes to be as large as possible. Therefore, lower distortion may also cause lower precision. To remove this imposed scaling, we introduce a scale-independent formulation of the distortion:

$$\text{disto}^{\text{scale-free}}(\pi, D) = \min_{s \in \mathbb{R}_+} \text{disto}(s \cdot \pi, D) \,, \tag{5}$$

where $s \cdot \pi$ are the scaled prototypes, whose coordinates in $\Omega$ are multiplied by a scalar factor $s$. As shown in the appendix, $\text{disto}^{\text{scale-free}}$ can be efficiently computed algorithmically.

**Distortion-Based Penalization** We propose to incorporate the error qualification $D$ into the prototypes' relative arrangement by encouraging a low *scale-free* distortion between $\pi$ and $D$. To this end, we define the following smooth surrogate of $\text{disto}^{\text{scale-free}}$:

$$\mathcal{L}_{\text{disto}}(\pi) = \frac{1}{K(K-1)} \min_{s \in \mathbb{R}_+} \sum_{k,l \in \mathcal{K}^2,\, k \neq l} \left( \frac{s d(\pi_k, \pi_l) - D[k,l]}{D[k,l]} \right)^2 \,. \tag{6}$$

$\mathcal{L}_{\text{disto}}$ can be computed in closed form as a function of $\pi$ and can thus be directly used as regularizer.

### 3.3 End-to-end Training

We combine $\mathcal{L}_{\text{data}}$ and $\mathcal{L}_{\text{disto}}$ in a single loss $\mathcal{L}$. $\mathcal{L}_{\text{data}}$ allows to jointly learn the embedding function $f$ and the class prototypes $\pi$, while $\mathcal{L}_{\text{disto}}$ enforces a metric-consistent prototype arrangement:

$$\mathcal{L}(f, \pi) = \mathcal{L}_{\text{data}}(f, \pi) + \lambda \mathcal{L}_{\text{disto}}(\pi) \,, \tag{7}$$

with $\lambda \in \mathbb{R}_+$ an hyper-parameter setting the strength of the regularization.

### 3.4 Choosing a Metric Space

Prototypical networks operating on $\Omega = \mathbb{R}^m$ typically use the squared Euclidean norm in the distance function, motivated by its quality as a Bregman divergence (Snell et al., 2017). However, we observe that defining $d$ with the Euclidean norm yields significantly better results. The non-differentiability

can be handled by composing with a Huber-like (Huber et al., 1973; Charbonnier et al., 1997) function $d = H(\|\cdot\|)$, with $H$ defined as:

$$H(x) = \delta(\sqrt{\|x\|^2/\delta^2 + 1} - 1) \ , \tag{8}$$

and $\delta \in \mathbb{R}_+$ a (small) hyper-parameter. The resulting metric $d$ is asymptotically equivalent to the Euclidean norm for large distances, and behaves like the smooth squared Euclidean norm for small distances. In Section 4.5, we investigate the effect of this change.

# 4 Experiments

## 4.1 Datasets and Backbones

We evaluate our approach with different tasks on public datasets with fine-grained class hierarchies: image classification on CIFAR100 (Krizhevsky et al., 2009) and iNaturalist-19 (Van Horn et al., 2018), RGB-D image segmentation on NYUDv2 (Nathan Silberman & Fergus, 2012), and image sequence classification on S2-Agri (Sainte Fare Garnot et al., 2020). We define the cost matrix of these class sets as the length of the shortest path between nodes in the tree-shape taxonomies, represented in the Appendix. As shown in Table 1, these datasets cover different settings in terms of data characteristics, as well as tree structures.

**Illustrative Example on MNIST:** In Figure 1 and Figure 3 of the Appendix, we illustrate the difference in performance and embedding organization for different approaches. We use a small 3-layer convolutional net trained on MNIST with random rotations (up to $40$ degrees) and affine transformations (up to $1.3$ scaling). For plotting convenience, we set the feature's dimension to $2$.

**Image Classification on CIFAR100:** CIFAR100 is composed of $50\,000$ training images and $10\,000$ test images of size $32 \times 32$, evenly distributed across $100$ classes. We use a super-class system inspired by Krizhevsky et al. (2009) and form a 5-level hierarchical nomenclature of size: $2$, $4$, $8$, $20$, and $100$ classes. We use as backbone the established ResNet-18 (He et al., 2016) for this dataset.

**Semantic Segmentation on NYUDv2:** NYUDv2 is an RGB-D image segmentation dataset composed of $1\,449$ pairs of RGB images of indoor scenes and their corresponding depth maps. We use the standard split of $795$ training and $654$ testing pairs. We combine the $4$ and $40$ class nomenclatures of Gupta et al. (2013) and the $13$ class system defined by Handa et al. (2016) to construct a 3-level hierarchy. We use FuseNet (Hazirbas et al., 2016) as backbone for this dataset.

**Image Sequence Classification on S2-Agri:** S2-Agri comprises $189\,971$ sequences of multi-spectral satellite images of agricultural parcels. We define a $4$-level hierarchy of size $4$, $12$, $19$, and $44$ classes to organize the crop types. This class hierarchy is critical to monitoring agencies, as it is related to the level of subsidy allocated to farmers. We use the PSE+TAE architecture (Sainte Fare Garnot et al., 2020) as the backbone, and follow their $5$-fold cross-validation scheme for training.

**Fine-Grained Image Classification on iNaturalist-19 (iNat-19)** iNat-19 (Van Horn et al., 2018) is a fine-grained image classification dataset comprised of $265\,213$ images of living organisms. The images are labeled by experts and users of the *iNaturalist* app, using a fine-grained taxonomy. iNat-19 contains $1\,010$ different classes, organized into a hierarchy of 7 levels with respective width $3$, $4$, $9$, $34$, $57$, $72$, and $1\,010$. We use ResNet-18 pre-trained on ImageNet as backbone. We sample $75\%$ of available images for training, while the rest is evenly split into a validation and test set.

## 4.2 Evaluated Methods and Hyper-Parameterization

The embedding space $\Omega$ is $\mathbb{R}^{512}$ for iNat-19 and $\mathbb{R}^{64}$ for all other datasets. We define $d$ as the Euclidean norm (see 4.5 for a discussion on this choice). We chose $\lambda = 1$ in (7) for all datasets. We use the same training schedules and learning rates as the backbone networks in their respective papers. In particular, the class imbalance of S2-Agri is handled with a focal loss (Lin et al., 2017).

We evaluate two variations of our approach to assess the benefit of its different components.

- **Metric-Guided Prototypes** (Guided-proto): Learnt prototypes with metric-guided regularization.
- **Free Prototypes** (Free-proto): Learnt prototypes without regularization: $\lambda = 0$ in (7).

Table 1: Data composition and nomenclature of the four studied datasets. IR stands for the Imbalance Ratio (largest over smallest class count), nodes and leaves denote respectively the total number of classes and leaf-classes in the tree-shape hierarchy, ABF stands for the Average Branching Factor, and $\langle D \rangle$ stands for the average pairwise distance.

| Dataset | Data | | Hierarchical Tree | | | |
|---|---|---|---|---|---|---|
| | Volume (Gb) | IR | Depth | Nodes (leaves) | ABF | $\langle D \rangle$ |
| NYUDv2 | 2.8 | 93 | 3 | 57 (40) | 5.0 | 4.3 |
| S2-Agri | 28.2 | 617 | 4 | 83 (45) | 5.8 | 6.5 |
| CIFAR100 | 0.2 | 1 | 5 | 134 (100) | 3.8 | 7.0 |
| iNat-19 | 82.0 | 31 | 7 | 1189 (1010) | 6.6 | 11.0 |

### 4.3 Competing methods

All the backbone networks presented in Section 4.1 use the cross-entropy loss for supervision in the paper in which they are introduced. The resulting performance of these networks serves as baseline to estimate the gains in Average Cost (AC) and Error Rate (ER) provided by our approach and other competing methods we re-implemented.

- **Hierarchical Cross-Entropy** (HXE) Bertinetto et al. (2020) model the class structure with a hierarchical loss composed of the sum of the cross-entropies at each level of the class hierarchy. As suggested, a parameter $\alpha$ taken as $0.1$ defines exponentially decaying weights for higher levels.
- **Soft Labels** (Soft-labels) Bertinetto et al. (2020) propose as second baseline in which the the one-hot target vectors are replaced by soft target vectors in the cross-entropy loss. These target vectors are defined as the softmin of the costs between all labels and the true label, with a temperature $1/\beta$ chosen as $0.1$, as recommended in Bertinetto et al. (2020).
- **Earth Mover Distance regularization** (XE+EMD): Hou et al. (2016) propose to account for the relationships between classes with a regularization based on the squared earth mover distance. We use $D$ as the ground distance matrix between the probabilistic prediction $p$ and the true class $y$:

$$\mathcal{L}_{EMD}(p, y) = \sum_{k=1}^{K} p_k^2 (D[k, y] - \mu) \ .$$

  This regularizer is added along the cross-entropy with a weight of $0.5$ and an offset $\mu$ of $3$.
- **Hierarchical Inference** (YOLO): Redmon & Farhadi (2017) propose to model the hierarchical structure between classes into a tree-shaped graphical model. First, the conditional probability that a sample belongs to a class given its parent class is obtained with a softmax restricted to the class' co-hyponyms (*i.e.* siblings). Then, the posterior probability of a leaf class is given by the product of the conditional probability of its ancestors. The loss is defined as the cross-entropy of the resulting probability of the leaf-classes.
- **Hyperspherical Prototypes** (Hyperspherical-proto): The method proposed by Mettes et al. (2019) is closer to ours, as it relies on embedding class prototypes. They advocate to first position prototypes on the hypersphere using a rank-based loss (see Section 4.5) combined with a prototype-separating term. They then use the squared cosine distance between the image embeddings and prototypes to train the embedding network. Note that in our re-implementation, we used the finite metric defined by $D$ instead of Word2Vec (Mikolov et al., 2013) embeddings to position prototypes. Lastly, we do not evaluate on S2-Agri as the integration of the focal loss is non-trivial.
- **Deep Mean Classifiers** (Deep-NCM): Guerriero et al. (2018) present another prototype-based approach. Here, the prototypes are the cumulative mean of the embeddings of the classes' samples, updated at each iteration. The embedding network is supervised with $\mathcal{L}_{\text{data}}$ with $d$ defined as the squared Euclidean norm.

### 4.4 Analysis

**Overall Performance:** As displayed in Figure 2, the benefits provided by our approach can be appreciated on all datasets. Compared to cross-entropy, our metric-guided prototype models improve the AC by $3\%$ on NYUDv2 and S2-Agri, and up to $9\%$ and $14\%$ for CIFAR100, and iNat-19 respectively. The hierarchical inference scheme of Redmon & Farhadi (2017) performs on par or

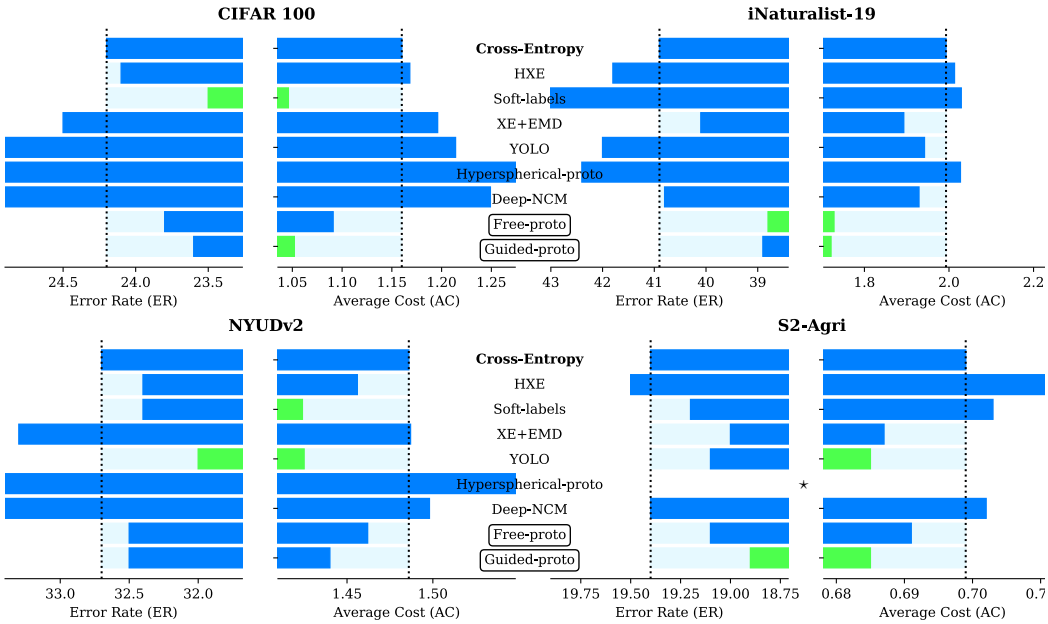


Figure 2: Error Rate (ER) in % and Average Cost (AC) on four datasets for our proposed methods (framed names), the Cross-Entropy baseline (in bold), and the competing approaches. The best performances on each dataset are plotted in green. Our guided prototype approach improves both the ER and AC across the four datasets. The metrics are computed with the median over 5 runs for CIFAR100, the average over 5 cross-validation folds for S2-Agri, and a single run for NYUDv2 and iNat-19. The numeric values are given in the Appendix. ($\star$ not evaluated on S2-Agri).

better than our methods for NYUDv2 and S2-Agri, while Soft-labels perform well on CIFAR100 and NYUDv2. Yet, only the metric guided prototype approach brings a consistent reduction of the hierarchical cost across the four datasets. This suggest that arranging the embedding space consistently with the cost metric is a robust way of reducing a model's hierarchical error cost.

While being initially designed to reduce the AC, our methods also improve the ER by 3 to 4% across all datasets compared to the cross-entropy baseline. This indicates that cost matrices derived from the class hierarchy can indeed help neural networks to learn better representations.

**Prototype Learning:** We observe that our unguided learnt prototype approach Free-proto outperforms the Deep-NCM method. This suggest that defining prototypes as the centroids of their class representations might actually be disadvantageous. As illustrated on Figure 1c, the positions of the embeddings follow a Voronoi partition (Fortune, 1992) with respect to the learnt prototypes rather than the prototypes being at the centroid of representations. A surprising observation for us is that Free-proto consistently outperforms the cross-entropy, both in terms of AC and ER.

**Computational Efficiency:** Computing distances to prototypes is comparable in terms of computation time to computing a linear mapping. Consequently, both training and inference time are equivalent when using the cross-entropy or guided-proto-disto, which is 2% faster.

### 4.5 Ablation Study

**Fixed-Scale Distortion:** In Table 2, we compare the performance of our *scale-free* regularizer to an alternative version of $\mathcal{L}_{\text{disto}}$ in which the scale remains fixed to $s = 1$. Across datasets, this results in an increased error rate, which we attribute to prototype distances being fixed by $\mathcal{L}_{\text{disto}}$.The benefit of our scale-free regularizer is especially valuable for the complex class structure of iNat-19, improving the overall classification accuracy by 1 point compared to the fixed-scale version.

Table 2: Influence of the choice of scaling in $\mathcal{L}_{\text{disto}}$, metric guiding regularizer, and distance function $d$ on the performance of Guided-proto on the four datasets. For $d$, we compare the performance of the Euclidean norm, the pseudo-Huberized Euclidean norm, and the square Euclidean norm.

| | CIFAR100 | | NYUDv2 | | S2-Agri | | iNat-19 | |
|---|---|---|---|---|---|---|---|---|
| | ER | AC | ER | AC | ER | AC | ER | AC |
| **Guided-proto** | 23.6 | **1.052** | 32.5 | 1.440 | **18.9** | **0.685** | **38.9** | 1.721 |
| Fixed-scale | +0.1 | +0.003 | 0.0 | 0.000 | +0.2 | **0.001** | +0.9 | 0.000 |
| Rank-based guiding | **-0.3** | +0.004 | +0.2 | +0.005 | +0.2 | +0.006 | +0.4 | **-0.003** |
| Fixed-proto | +1.1 | +0.031 | +0.6 | +0.013 | +0.5 | +0.025 | +5.0 | +0.427 |
| Pseudo-Huber | +0.1 | +0.015 | **-0.3** | **-0.017** | +0.4 | +0.016 | +0.2 | +0.003 |
| Squared Norm | +1.0 | +0.118 | 0.0 | +0.005 | +0.6 | +0.022 | +2.2 | +0.233 |

**Rank-based Regularization:** Mettes et al. (2019) use a rank-based loss (Burges et al., 2005) to encourage prototype mappings whose pairwise distance follows the same order as an external qualification of errors $D$. We argue that our formulation of $\mathcal{L}_{\text{disto}}$ provides a stronger supervision than only considering the order of distances, and allows the prototypes to find a more profitable arrangement in the embedding space. In Table 2, we observe that replacing our distortion-based loss by a rank-based one results in a slight decrease of overall performance.

**Guiding Schedule:** Our experiments confirm the benefit of jointly learning the prototypes and the embedding network instead of learning the prototypes first as Hyperspherical-proto. We also evaluate the performance of Fixed-proto in Table 2, for which we first fix the prototypes with $\mathcal{L}_{\text{disto}}$ and then train the network with $\mathcal{L}_{\text{data}}$. While this approach reduces the AC compared to the cross-entropy baseline in some cases, its ER is consistently higher than for guided methods. This suggests that insights from the data distribution can conversely benefit the positioning of prototypes.

**Choice of distance :** In Table 2, we report the performance of the Guided-proto model on the four datasets when replacing the Euclidean norm alternately with the squared Euclidean norm and an Huberized Euclidean distance (with $\delta = 0.1$ in (8)). Across our experiments, the squared-norm based model yields a worse performance. This is a notable result as it is the distance commonly used in most prototypical networks (Snell et al., 2017; Guerriero et al., 2018). The Huberized norm performs worse than the Euclidean distance on all dataset, with the exception NYUDv2.

**Further Ablation Study:** In the Appendix we present an extended ablation study, notably showcasing the resilience of our approach to a wide-range of hyper-parameters value.

## 5 Conclusion

We introduced a new prototype-based framework, incorporating a qualification of errors through a metric-based regularization. We showed that our methods consistently decreased the average cost of three different backbone networks on different tasks and datasets. Furthermore, our approach can reduce the rate of errors as well. A PyTorch implementation of our framework as well as an illustrative notebook are available at `https://github.com/mgp-anon/metric-guided-prototype` (repository anonymized for review).

This work, along with other recent investigations (Bertinetto et al., 2020), highlights the interest of modeling hierarchical class structures in modern deep networks. Beyond the decrease in prediction costs, such hierarchies can lead to an improved overall performance. This calls for further investigation into the mechanisms by which semantic class structures can benefit the learning of expressive representations. Among other promising avenues for further research, we plan to investigate the use of non-Euclidean embedding spaces, which are known to be well-suited for embedding hierarchies, and the generalization of our framework to regression tasks.

## REFERENCES


Naveed Akhtar and Ajmal Mian. Threat of adversarial attacks on deep learning in computer vision: A survey. *IEEE Access*, 2018.

Shahanaz Ayub and JP Saini. ECG classification and abnormality detection using cascade forward neural network. *International Journal of Engineering, Science and Technology*, 2011.

Luca Bertinetto, Romain Mueller, Konstantinos Tertikas, Sina Samangooei, and Nicholas A Lord. Making better mistakes: Leveraging class hierarchies with deep networks. In *CVPR*, 2020.

Jean Bourgain. On Lipschitz embedding of finite metric spaces in Hilbert space. *Israel Journal of Mathematics*, 1985.

Chris Burges, Tal Shaked, Erin Renshaw, Ari Lazier, Matt Deeds, Nicole Hamilton, and Greg Hullender. Learning to rank using gradient descent. In *ICML*, 2005.

Pierre Charbonnier, Laure Blanc-Féraud, Gilles Aubert, and Michel Barlaud. Deterministic edge-preserving regularization in computed imaging. *IEEE Transactions on Image Processing*, 1997.

Christopher De Sa, Albert Gu, Christopher Ré, and Frederic Sala. Representation tradeoffs for hyperbolic embeddings. In *Proceedings of Machine Learning Research*, 2018.

Jia Deng, Alexander C Berg, Kai Li, and Li Fei-Fei. What does classifying more than 10,000 image categories tell us? In *ECCV*, 2010.

Nanqing Dong and Eric Xing. Few-shot semantic segmentation with prototype learning. In *BMVC*, 2018.

Steven Fortune. Voronoi diagrams and Delaunay triangulations. In *Computing in Euclidean Geometry*. World Scientific, 1992.

Andrew Gelman, John B Carlin, Hal S Stern, David B Dunson, Aki Vehtari, and Donald B Rubin. *Bayesian data analysis*. CRC press, 2013.

Samantha Guerriero, Barbara Caputo, and Thomas Mensink. DeepNCM: deep nearest class mean classifiers. In *ICLR, Worskhop*, 2018.

Saurabh Gupta, Pablo Arbelaez, and Jitendra Malik. Perceptual organization and recognition of indoor scenes from RGB-D images. In *CVPR*, 2013.

A Handa, V Patraucean, V Badrinarayanan, S Stent, and R Cipolla. Uunderstanding real world indoor scenes with synthetic data. In *CVPR*, 2016.

Caner Hazirbas, Lingni Ma, Csaba Domokos, and Daniel Cremers. Fusenet: Incorporating depth into semantic segmentation via fusion-based CNN architecture. In *ACCV*, 2016.

Kaiming He, Xiangyu Zhang, Shaoqing Ren, and Jian Sun. Deep residual learning for image recognition. In *CVPR*, 2016.

Le Hou, Chen-Ping Yu, and Dimitris Samaras. Squared earth mover's distance-based loss for training deep neural networks. In *NeurIPS workshop on learning on distributions, functions, graphs and groups*, 2016.

Peter J Huber et al. Robust regression: asymptotics, conjectures and monte carlo. *The Annals of Statistics*, 1973.

Piotr Indyk, Jiří Matoušek, and Anastasios Sidiropoulos. Low-distortion embeddings of finite metric spaces. In *Handbook of discrete and computational geometry*. Chapman and Hall/CRC, 2017.

Saumya Jetley, Bernardino Romera-Paredes, Sadeep Jayasumana, and Philip Torr. Prototypical priors: From improving classification to zero-shot learning. In *BMVC*, 2015.

Aris Kosmopoulos, Ioannis Partalas, Eric Gaussier, Georgios Paliouras, and Ion Androutsopoulos. Evaluation measures for hierarchical classification: a unified view and novel approaches. *Data Mining and Knowledge Discovery*, 2015.

Alex Krizhevsky, Geoffrey Hinton, et al. Learning multiple layers of features from tiny images. Technical report, University of Toronto, 2009.

Tsung-Yi Lin, Priya Goyal, Ross Girshick, Kaiming He, and Piotr Dollár. Focal loss for dense object detection. In *ICCV*, 2017.

Pascal Mettes, Elise van der Pol, and Cees Snoek. Hyperspherical prototype networks. In *NeurIPS*, 2019.

Tomas Mikolov, Kai Chen, Greg Corrado, and Jeffrey Dean. Efficient estimation of word representations in vector space. In *ICLR Workshop*, 2013.

George A Miller, Richard Beckwith, Christiane Fellbaum, Derek Gross, and Katherine J Miller. Introduction to wordnet: An on-line lexical database. *International Journal of Lexicography*, 1990.

Pushmeet Kohli Nathan Silberman, Derek Hoiem and Rob Fergus. Indoor segmentation and support inference from RGBD images. In *ECCV*, 2012.

Joseph Redmon and Ali Farhadi. YOLO9000: better, faster, stronger. In *CVPR*, 2017.

Deboleena Roy, Priyadarshini Panda, and Kaushik Roy. Tree-CNN: a hierarchical deep convolutional neural network for incremental learning. *Neural Networks*, 2020.

Olga Russakovsky, Jia Deng, Hao Su, Jonathan Krause, Sanjeev Satheesh, Sean Ma, Zhiheng Huang, Andrej Karpathy, Aditya Khosla, Michael Bernstein, et al. Imagenet large scale visual recognition challenge. *International Journal of Computer Vision*, 2015.

Vivien Sainte Fare Garnot, Loic Landrieu, Sebastien Giordano, and Nesrine Chehata. Satellite image time series classification with pixel-set encoders and temporal self-attention. In *CVPR*, 2020.

Ruslan Salakhutdinov, Joshua B Tenenbaum, and Antonio Torralba. Learning with hierarchical-deep models. *IEEE Transactions on Pattern Analysis and Machine Intelligence*, 2012.

Carlos N Silla and Alex A Freitas. A survey of hierarchical classification across different application domains. *Data Mining and Knowledge Discovery*, 2011.

Jake Snell, Kevin Swersky, and Richard Zemel. Prototypical networks for few-shot learning. In *NeurIPS*, 2017.

Nitish Srivastava and Russ R Salakhutdinov. Discriminative transfer learning with tree-based priors. In *NeurIPS*, 2013.

Robert Tibshirani, Trevor Hastie, Balasubramanian Narasimhan, and Gilbert Chu. Diagnosis of multiple cancer types by shrunken centroids of gene expression. *Proceedings of the National Academy of Sciences*, 2002.

Grant Van Horn, Oisin Mac Aodha, Yang Song, Yin Cui, Chen Sun, Alex Shepard, Hartwig Adam, Pietro Perona, and Serge Belongie. The iNaturalist species classification and detection dataset. In *CVPR*, 2018.

Zhicheng Yan, Hao Zhang, Robinson Piramuthu, Vignesh Jagadeesh, Dennis DeCoste, Wei Di, and Yizhou Yu. HD-CNN: hierarchical deep convolutional neural networks for large scale visual recognition. In *ICCV*, 2015.